Environmental Science & Technology

pubs.acs.org/est

Article

Light-Enhanced Heterogeneous Conversion of NO_2 to HONO on Solid Films Consisting of Fluorene and Fluorene/Na_2SO_4: An Impact on Urban and Indoor Atmosphere

Jiangping Liu, Huifan Deng, Sheng Li, Haoyu Jiang, Majda Mekic, Wentao Zhou, Yiqun Wang, Gwendal Loisel, Xinming Wang, and Sasho Gligorovski*

Cite This: *Environ. Sci. Technol.* 2020, 54, 11079−11086

Read Online

ACCESS | Metrics & More | Article Recommendations | Supporting Information

ABSTRACT: Polycyclic aromatic hydrocarbons (PAHs) as constituents of urban grime and indoor surfaces can impact the photochemical conversion of nitrogen dioxide (NO_2) to nitrous acid (HONO) thereby impacting the oxidation capacity of the atmosphere. In this study we investigate the effect of relative humidity (RH%), light intensity, and NO_2 concentrations on uptake coefficients (γ) of NO_2 on solid film consisting of fluorene (FL) and a mixture of FL and Na_2SO_4 as a proxy for urban and indoor grime at ambient pressure and temperature. $\gamma(NO_2)$ on solid FL increased markedly from $(5.7 \pm 1.7) \times 10^{-7}$ at 0% RH to $(4.6 \pm 1.0) \times 10^{-6}$ at 90% RH. The NO_2 to HONO conversion yield, $(\Delta HONO/\Delta NO_2)$%, increases with RH from 40% at 0% RH up to 80% at 60−90% RH, indicating that the water molecules favor the formation of HONO up to 60% RH. These results suggest that the heterogeneous photochemical reaction of NO_2 on FL and FL/Na_2SO_4 can be an important source of HONO in the urban environment and indoor atmosphere and should be considered in photochemical models.

1. INTRODUCTION

Urban surfaces such as windows and walls are ubiquitous in the urban environment. A thin film with a thickness from 10 to 1000 nm can develop on urban surfaces as grime.[1−3] Urban grime consists of an important number of chemical compounds,[4,5] emitted into the atmosphere by vehicles, factories, and a host of other sources. Gingrich et al.[6] were the first to suggest that urban grime could be considered as a separate environmental compartment. The presence of complex and potentially light-absorbing organic compounds within urban grime can affect photochemical processes on impervious urban surfaces which in turn can have an impact on urban air quality. Polycyclic aromatic hydrocarbons (PAHs) represent an important class of organic compounds accounting for approximately 20% of the organic mass of urban grime.[5,7] The highest concentration of total PAHs, predominantly fluorene, phenanthrene, fluoranthene, and pyrene, was found to be 1.4 $\mu g\ m^{-2}$ on urban grime collected from window surfaces in two large cities in southern China, Guangzhou and Hong Kong.[8] These authors reported that PAHs were adsorbed on indoor windows as well.[8] For lightweight PAHs, such as fluorene, indoor/outdoor ratios were reported to be close to 1.0, and in some cases, the ratios were higher than 1.0, indicating that these compounds can also play a role in indoor air.[8] Similar concentrations of adsorbed PAHs on urban grime in Toronto and Stockholm were also reported.[6,9] Wide electron delocalization in PAH molecules allows them to absorb sunlight and initiate photochemical processes on urban and indoor surfaces.[10,11] In addition to the organic composition, urban grime is also loaded with salts such as sulfate which is very stable within the film.[1] Sulfates on urban grime can be formed through reaction of gaseous SO_2 with sodium and calcium, yielding Na_2SO_4 and $CaSO_4$, respectively.[1,12,13]

Donaldson and co-workers[1,2,14] have shown that there is a potential for significant recycling of NO_2 and/or HONO into the atmosphere from urban grime, which can affect ozone and OH radical formation in the urban atmosphere. A number of studies have shown that the uptake coefficients of NO_2 on simulated urban grime are enhanced in the presence of light irradiation, yielding high amounts of HONO.[15−19] A recent study demonstrated enhanced NO_2 uptake coefficients and HONO formation yields on real urban grime collected in downtown Guangzhou, China.[20] Key parameters that influence

Received: April 26, 2020
Revised: June 25, 2020
Accepted: June 29, 2020
Published: June 29, 2020

https://dx.doi.org/10.1021/acs.est.0c02627
Environ. Sci. Technol. 2020, 54, 11079−11086

NO_2 heterogeneous reactions are the intensity of light irradiation, relative humidity (RH%), temperature, and NO_2 concentration.[20−30]

Here we investigate the influence of RH%, light intensity, and NO_2 concentration on the heterogeneous NO_2 to HONO conversion on solid FL and a mixture of FL and Na_2SO_4 in a flow tube photoreactor simultaneously coupled to long path absorption photometer (LOPAP) and NOx analyzers for online measurements of HONO and (NO + NO_2), respectively.

This study shows that uptake coefficients of NO_2 on solid FL films are enhanced under light irradiation and increase nonlinearly as a function of RH. HONO formation yields increase with RH as well. The presence of Na_2SO_4 diminishes the NO_2 uptake coefficients and HONO yields. The reaction pathway of HONO formation and its potential implications on oxidation capacity of the urban atmosphere are discussed.

2. MATERIALS AND METHODS

2.1. Samples. The solid films were prepared before each experiment by dissolving 0.05 g of FL (Sigma-Aldrich, China) into 10 mL of dichloromethane (DCM) (Macklin, China) and sonicating with an ultrasonic instrument about 10 min to accelerate dissolution. Then the solution was gently applied with a syringe on a rectangular borosilicate glass plate (45 cm length × 1.5 cm width). FL/Na_2SO_4 mixed films were prepared following the same procedure by depositing 0.05 g of FL and 0.05 g of Na_2SO_4(Macklin, China) dissolved in DCM solution on the glass plates. The glass plates were rinsed with ultrapure water provided by Sartorius (18 M-ohm, H_2O-MM-UV-T, Germany), and then they were dried in an oven (105 °C) overnight to remove residual water.

2.2. Flow Tube Reactor. The flow tube reactor is made up of a cylindrical borosilicate glass tube placed into a double-wall glass tube (50 cm length and 2.6 cm inner diameter) connected to a thermostatic bath (Lauda RC6 refrigerated bath with RCS thermostat, temperature accuracy = ±0.02 K at 263 K) which allowed operation at constant temperature, 296 K. The glass plate previously coated with solid FL film or FL/Na_2SO_4 was placed in the flow tube reactor exposed to four lamps (Philips 20 W) suspended perpendicularly above the reactor with continuous emission in the range of 300−400 nm. The resulting spectral intensities of the lamps were measured by calibrated spectroradiometer (Ocean Optics, USA) coupled with a linear-array CCD detector.

All the experiments described here were performed under atmospheric pressure at constant temperature 296 ± 1 K, and the relative humidity (RH) ranged from 0% to 90%. The RH in the flow tube reactor was controlled by introducing a constant flow of N_2 gas to a bubbler filled with deionized water. The temperature and the RH of the gas flows were measured by using an HMT330 Sensor (Vaisala, Finland, ±2% accuracy).

A standard gas bottle of NO_2 (10 ppmv in N_2, Messer Gases Co., Ltd.) in high purity nitrogen (99.99%, Messer Gases Co., Ltd.) was used for these experiments. The gas inlet system was connected to a mixing tube to allow two successive dilutions to obtain atmospherically relevant 40 ppb of NO_2 which was used for most of the experiments. To assess the dependence of uptakes coefficients on different NO_2 mixing ratios, the range of employed NO_2 mixing ratios was 20−125 ppb. The desired quantity of NO_2 was introduced to the flow tube reactor by a movable glass made injector. For the first dilution, a constant flow of 10 mL min^{-1} of NO_2 (Horiba Metron Series mass flow controller, ±1% accuracy) flow was mixed with 200 mL min^{-1} high purity nitrogen flow. Then a sheath flow of 1000 mL min^{-1} used for the bubbler was also incorporated in the reactor to get the second dilution. All gases were taken directly from gas cylinders without further purification prior to use.

2.3. NO_x and HONO Measurements. During the experiments the NO_2 signal was measured by a chemiluminescence instrument (Eco Physics, model CLD 88p) connected to a photolytic (metal halide lamp) converter (Eco Physics, model PLC 860). The detection limit of NO_x analyzer is 10 ppt and a time resolution of 1 s.

The detection of HONO was performed by a LOng Path Absorption Photometer (LOPAP, QUMA Elektronik & Analytik, Wuppertal, Germany) with a detection limit <30 ppt for a resolution time about 2.5 min under the operation conditions applied (gas flow 1 L/min). A detailed description of its operation procedure and principle can be found in the literature.[31−33]

2.4. Ion Analysis. Ion analysis was carried out to measure the water-soluble ions. Briefly, each piece of glass plate was extracted with 5 mL of Milli-Q quality water and sonicated by using an ultrasonic bath for 2 min and then rinsed twice on each side with 5 mL of ultrapure water, for a total extraction volume of 10 mL. The extracts were filtered through a 0.22 μm IC Millex-LG filter and then stored in a precleaned HDPE bottle. Samples of 1 mL were injected onto an analytical column of an ion-chromatography system (Metrohm, 883 Basic IC plus).

2.5. Kinetic Analysis. The kinetic behavior of the light-induced heterogeneous reaction between NO_2 and FL or FL/Na_2SO_4 was fitted by pseudo-first-order kinetic rate law with respect to the gas-phase NO_2 concentration. The first-order rate coefficient, k_{1,NO_2}, can be described as follows:

$$k_{1,NO_2} = \frac{\ln(C_0/C)}{t} \quad (1)$$

where C_0 is the initial NO_2 concentration which corresponds to the situation when there is no contact between the coated surface and gaseous NO_2, C represents the concentration of NO_2 following the reaction with the coated glass surface, whereas t is the residence time of NO_2 in the reactor.

The geometric uptake coefficient of NO_2 (γ_{NO_2}) defines the reaction probability of gas-phase NO_2 with the adsorbed FL or FL/Na_2SO_4 on the glass surface. In this study the reactive uptake of NO_2 was estimated as follows:

$$\gamma_{NO_2} = \frac{4 \times k_{1,NO_2}}{\overline{V_{NO_2}} \times A} \quad (2)$$

where k_{1,NO_2} is the observed pseudo-first-order rate constant for the reaction between NO_2 and the coated glass surface, $\overline{V_{NO_2}}$ is the average molecular speed of NO_2, and A describes the geometry of the reactor as a ratio between the reactive surface (S) of the glass plate and the volume of the reactor (V).[20]

The geometric uptake coefficient was applied in this study instead of uptake coefficient based on "BET surface area" because the latter is more appropriate for highly porous surfaces (soil, mineral dust) which is not the case here.[20]

The Cooney−Kim−Davis method was applied to correct the measured uptake coefficients for gas-phase diffusion. The

https://dx.doi.org/10.1021/acs.est.0c02627
Environ. Sci. Technol. 2020, 54, 11079−11086

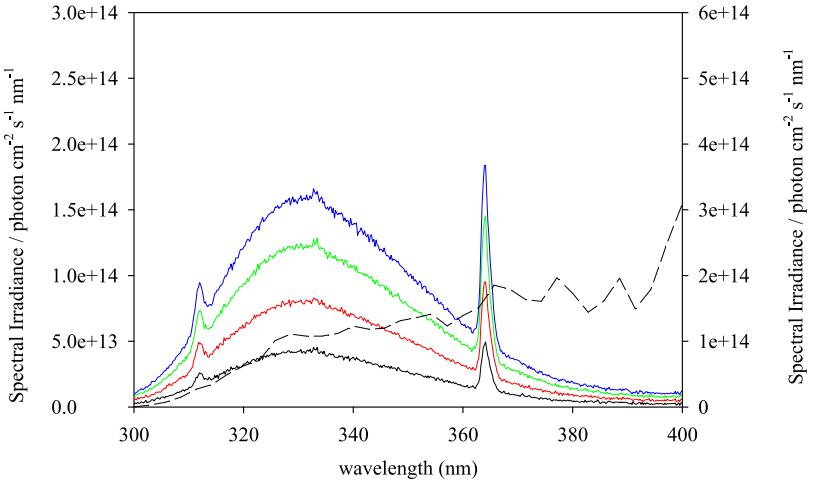

Figure 1. Comparison of the spectral irradiance of different UV−vis lamps and the spectral irradiance of the sunlight (long dash line) determined by the TUV model. Solid black, red, green, and blue lines correspond to the measured spectral irradiance of 1, 2, 3, and 4 UV−vis lamps, respectively. The spectral irradiance is determined for Guangzhou (latitude 23.12899, longitude 113.12899), solar zenith angle (SZA) 56.10° on October 3, 2019, at noon.

diffusion coefficient D was calculated by the Fuller method.[34] The correction of the uptake coefficient is around 3%.

3. RESULTS AND DISCUSSION

3.1. Spectral Irradiance. The measured spectral irradiance of different UV−vis lamps is shown in Figure 1. For comparison purposes, the spectral irradiance estimated according to the tropospheric ultraviolet and visible (TUV) model (TUV version 5.3)[35] is also shown in Figure 1. The UV fraction of the sunlight was derived from the lower boundary layer of the atmosphere span in the range from 300 to 400 nm. Although the profiles of the emission spectra between the lamps and the sunlight are not the same, the total integrated irradiance 2.6×10^{15} photons cm^{-2} s^{-1} in the wavelength region 300−400 nm emitted by four lamps is similar to the corresponding spectral irradiance of the sunlight (4.4×10^{15} photons cm^{-2} s^{-1}).

3.2. Effect of RH. The reactive uptakes of NO_2 were investigated as a function of different RH at 296 K (Figure 2). The uptake coefficients exhibit an untypical nonlinear increase with the RH similar to the dependence of $\gamma(NO_2)$ on solid films of anthrarobin, gentisic acid, and tannic acid.[18,36] The elevated NO_2 uptake coefficients on solid anthrarobin with increasing RH were associated with an acid−base equilibrium followed by an electron transfer which was the main mechanism of HONO formation.[36] In the case of gentisic acid and tannic acid, the surface-absorbed water facilitates the abstraction of a proton from the reaction intermediate (phenoxy-type radical).[18] Sosedova et al.[18] suggested that at high RH, considerably higher hydration of the organic coating occurs, implying decreased viscosity. For this reason, the bulk of the organic film becomes more accessible for the heterogeneous reaction which leads to higher NO_2 uptakes on a film consisting of FL, at higher RH. Fluorene does not contain OH groups, therefore pointing toward an alternative pathway involving a light-induced process (see Reaction Mechanism). In both cases, FL and FL/Na_2SO_4, there is almost no dependence of $\gamma(NO_2)$ up to 30% RH followed by a sharp increase of $\gamma(NO_2)$ at higher RH. It seems that at higher RH, surface-bound water acts as a H^+ donor on the electronically excited FL, thereby promoting the heterogeneous reaction of NO_2 with FL at higher RH. The increase of the NO_2 uptake coefficients on a solid film consisting of FL/Na_2SO_4 can be ascribed to enhanced hygroscopicity at higher RH which in turn makes the solid film more deliquescent. Therefore, it is most likely that at higher RH, the salting out effect makes FL more accessible for the reaction with NO_2, yet not enough to reach the NO_2 uptake on a film of pure FL. The salting out effect was previously observed for the heterogeneous reaction of ozone (O_3) with pyruvic acid.[37]

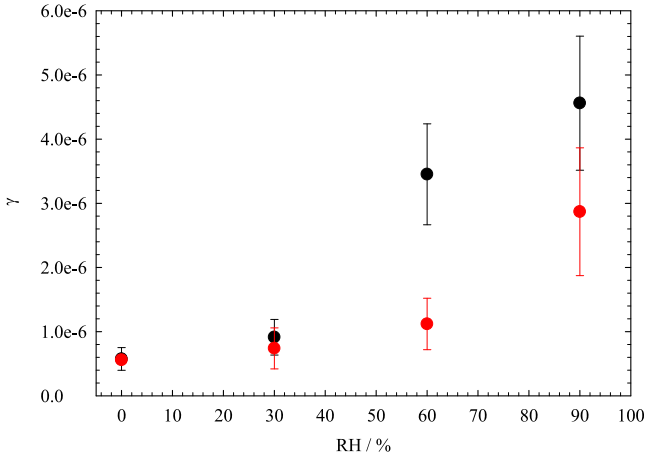

Figure 2. NO_2 uptake coefficients on (black dot) FL and (red dot) FL/Na_2SO_4, as a function of RH at NO_2 mixing ratio of 40 ppb, and light irradiation (15.5 W m^{-2}, 2.6×10^{15} photons cm^{-2} s^{-1}; 300 nm < λ < 400 nm). The error bars are derived from the uncertainties associated with the estimation of the uptake coefficients.

The reactive uptake coefficients, ($\gamma(NO_2)$), on solid FL ranged from $(5.7 \pm 1.7) \times 10^{-7}$ to $(4.6 \pm 1.0) \times 10^{-6}$ under light irradiation (15.5 W m^{-2}, 2.6×10^{15} photons cm^{-2} s^{-1}; 300 nm < λ < 400 nm). Figure 2 shows that the reactive uptakes of NO_2 on FL under light irradiation increased 8 times from $(5.7 \pm 1.7) \times 10^{-7}$ at 0% RH to $(4.6 \pm 1.0) \times 10^{-6}$ at 90% RH. The uptake coefficients of NO_2 on FL/Na_2SO_4 were slightly lower, ranging from $(5.6 \pm 0.1) \times 10^{-7}$ at 0% RH to $(2.9 \pm 0.9) \times 10^{-6}$ at 90% RH. These values are on the same order as the reactive uptakes of NO_2 on simulated urban grime

https://dx.doi.org/10.1021/acs.est.0c02627
Environ. Sci. Technol. 2020, 54, 11079−11086

consisting of fluoranthene/KNO_3, $\gamma(NO_2) = 6.6 \times 10^{-7}$ at 35% RH and phenantrene/KNO_3, $\gamma(NO_2) = 7.8 \times 10^{-7}$ at 35% RH[19] and in good agreement with the reactive uptakes on real urban grime, $\gamma(NO_2) = (1.1 \pm 0.2) \times 10^{-6}$ at 0% RH to $(5.8 \pm 0.7) \times 10^{-6}$ at 90% RH (0–90% RH) under light irradiation (2.6×10^{15} photons cm^{-2} s^{-1}; 300 nm < λ < 400 nm).[20]

NO_2 can be photolyzed with unit quantum yield in the wavelength region emitted by the lamps (300–400 nm) used in this study. The photolysis rate of NO_2, ($J(NO_2)$), in a clean flow tube reactor under the experimental conditions applied in this study ranged from 1.4×10^{-4} (s^{-1}) to 5.5×10^{-4} (s^{-1}), implying that NO_2 degradation due to its photolysis was negligible (0.1–0.6%) to the total NO_2. In addition, control experiments confirmed that there is no ozone production at the exit of the reactor by coupling an ozone analyzer with the flow tube reactor.

3.3. Influence of Light Intensity. The effect of light intensity on the NO_2 uptake coefficients was also explored by changing the number of lamps mounted above the flow-tube reactor. Figure 3 shows a linear dependence of the uptake

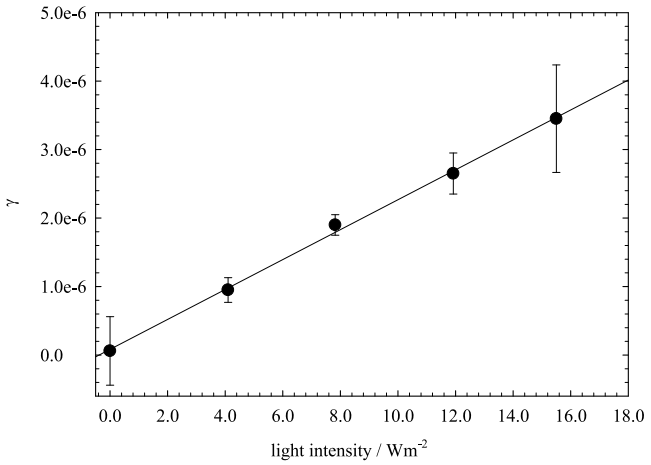

Figure 3. NO_2 uptake coefficients as a function of the photon flux at NO_2 mixing ratio of 40 ppb and 60% RH. The error bars are derived from the uncertainties associated with the estimation of the uptake coefficients.

coefficients of NO_2 with respect to the light intensity at an initial NO_2 mixing ratio of 40 ppb and 60% RH.

$$\gamma = (8.3 \pm 3.5) \times 10^{-8} + (2.2 \pm 0.06) \times 10^{-7} \times \text{light intensity (W m}^{-2}) \quad (3)$$

where $r = 0.99$.

The extrapolated NO_2 uptake coefficient on FL adsorbed on urban grime at a light intensity of 46 W m^{-2} for the wavelength range between 300 and 400 nm, which corresponds to a solar zenith angle of 48° as given by National Renewable Energy Laboratory (NREL),[38] would be 1×10^{-5}. This value is in good agreement with the uptake coefficient of NO_2 on humic acid (1×10^{-5}) under irradiation intensity of 400 W/m^2 (λ = 400–700 nm, 48° solar zenith angle), NO_2 mixing ratio of 30 ppb, temperature of 298 K, and RH of 30%.[39] However, the obtained uptake coefficient of 1×10^{-5} under realistic irradiation conditions is higher than the uptake coefficients of NO_2 on other PAHs such as pyrene, $\gamma = 8.8 \times 10^{-6}$,[17] at 50 ppb of NO_2, and fluoranthene, $\gamma = 1 \times 10^{-6}$,[19] at 20 ppb of NO_2. The uptake coefficient from this study is also about 1 order of magnitude higher than the uptake coefficient of NO_2 on gentisic acid ($\gamma = 1.6 \times 10^{-6}$)[18] which was used as a proxy for soot, at NO_2 mixing ratio of 20 ppb and 20% RH, under simulated light irradiation at 40° solar zenith angle.

3.4. Effect of NO_2 Mixing Ratios. Figure 4 shows the effect of NO_2 mixing ratios on the reactive uptake coefficient of

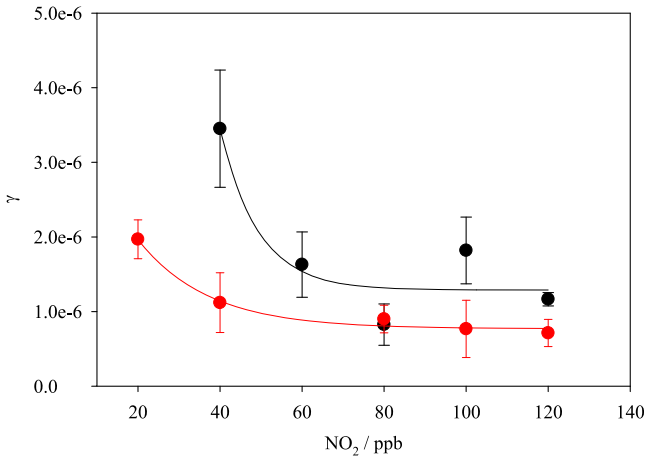

Figure 4. Uptake coefficients of NO_2 on solid FL (black circles) and FL/Na_2SO_4 (red circles) as a function of the initial NO_2 mixing ratios under light irradiation (15.5 W m^{-2}, 2.6×10^{15} photons cm^{-2} s^{-1} nm^{-1}) and 60% RH. The regression line shows the fit of the data to an inverse function of [NO_2], as implied by the Langmuir–Hinshelwood mechanism.

solid FL and FL/Na_2SO_4. In this case, the NO_2 loss decreases with increasing NO_2 mixing ratio. In both cases, the $\gamma(NO_2)$ is about 3 times higher and decreases with increasing mixing ratio of NO_2, from 3.2×10^{-6} at 40 ppb to 1.1×10^{-6} at 120 ppb of NO_2 for FL, and from 2.0×10^{-6} at 20 ppb to 7.1×10^{-7} at 120 ppb of NO_2 in case of FL/Na_2SO_4. The curve drawn through the points shows a fit of the data to an inverse function of the NO_2 mixing ratio according to eq S4.

An inverse dependence of the uptake coefficients on the mixing ratios of NO_2 was reported in few previous studies.[16,17,19] This kinetic behavior is consistent with a Langmuir–Hinshelwood mechanism, where the NO_2 partitions between the gas phase and the surface, and the surface reaction takes place between the coadsorbed NO_2 and FL or FL/Na_2SO_4.

Figure 5 shows the inverse dependence of the uptake coefficients as a function of the initial NO_2 concentration expressed in molecules cm^{-3}, consistent with the Langmuir–Hinshelwood mechanism followed by a plateau around 100 ppb ($\gamma = 1.8 \times 10^{-6}$) which can be ascribed to the saturation effect of the available adsorption sites on the coated glass plate.

A plot of $1/\gamma(NO_2)$ versus the NO_2 concentration is linear, confirming the Langmuir–Hinshelwood behavior of the kinetic data (see SI for details). The linear fit of the kinetic data for FL and FL/Na_2SO_4 is presented with eq 4 and eq 5, respectively:

$$1/\gamma = (2.4 \pm 0.2) \times 10^{-7} \times [NO_2] \text{ (molecules cm}^{-3}) + (1.8 \pm 0.3) \times 10^5 \quad (4)$$

where $r = 0.99$.

https://dx.doi.org/10.1021/acs.est.0c02627
Environ. Sci. Technol. 2020, 54, 11079–11086

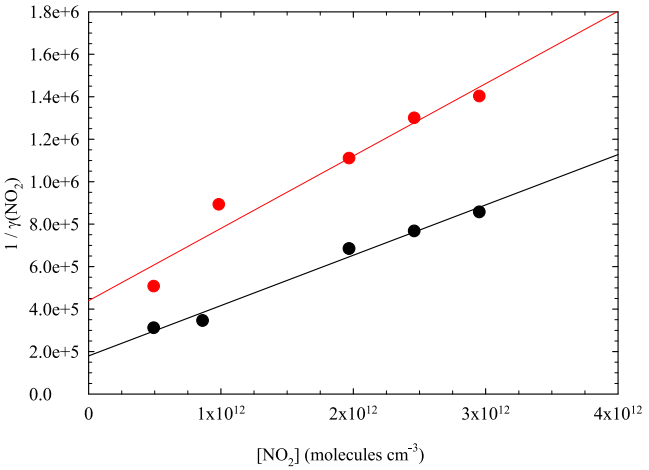

Figure 5. Linear dependence of the inverse uptake coefficients as a function of initial NO_2 concentration under light irradiation (15.5 W m^{-2}, 2.6 × 10^{15} photons cm^{-2} s^{-1} nm^{-1}) and 60% RH. Red circles correspond to FL/Na_2SO_4, and black circles correspond to FL.

$$1/\gamma = (3.4 \pm 0.5) \times 10^{-7} \times [NO_2]\ (\text{molecules cm}^{-3}) + (4.4 \pm 0.9) \times 10^{5} \quad (5)$$

where $r = 0.95$.

From eq S6, and eqs 4 and 5, the Langmuir adsorption constants (K_{NO_2}) on the solid film of FL and FL/Na_2SO_4 are estimated as 1.1 × 10^{-12} cm^3 $molecules^{-1}$ and 7.7 × 10^{-13} cm^3 $molecules^{-1}$, respectively, at 60% RH. For comparison, K_{NO_2} for the heterogeneous reaction of NO_2 on humic acid (HA)[39] and gentisic acid (GA)[18] under light irradiation was reported as 7.9 × 10^{-13} cm^3 $molecules^{-1}$ and 8.1 × 10^{-13} cm^3 $molecules^{-1}$, respectively. Thus, the K_{NO_2} value with respect to FL/Na_2SO_4 is in good agreement with the reported K_{NO_2} values for HA and GA. The slightly higher K_{NO_2} value in the case of FL film indicates that gaseous NO_2 adsorbs stronger on the FL surface than on the HA or GA surface, although the reaction mechanisms may be quite different.

3.5. HONO and NO Formation Yields. The yield of the NO_2 conversions of the two gas-phase products, HONO and NO, released during the light-induced heterogeneous reactions of NO_2 as a function of RH for both solid films FL and FL/Na_2SO_4, are presented in Table 1. The HONO and NO formation yields were calculated as a ratio of $\Delta HONO/\Delta NO_2$ and $\Delta NO/\Delta NO_2$, respectively. HONO was the major gas-phase product compound that emerged from the heterogeneous reaction of NO_2 on both FL and FL/Na_2SO_4, while the light-induced conversion of NO_2 to NO was a minor reaction pathway.

Table 1. Formed HONO and NO Yields under Light Irradiation (15.5 W m^{-2}, 2.6 × 10^{15} Photons cm^{-2} s^{-1} nm^{-1}) at Different RH, at 40 ppb of NO_2 and 296 K

	fluorene		fluorene/Na_2SO_4	
RH (%)	HONO yield (%)	NO yield (%)	HONO yield (%)	NO yield (%)
0	40.31	7.94	29.23	20.58
30	66.16	17.05	27.06	38.65
60	80.32	8.68	13.08	9.37
90	80.87	15.08	27.79	11.62

As shown in Table 1, the HONO yield formed on the FL surface increases with RH, reaching a plateau at 60−90% RH and indicating that the water molecules favor the formation of HONO up to 60% RH. On the other hand, the HONO yield formed by light-induced heterogeneous conversion of NO_2 on a mixture of FL/Na_2SO_4 is independent of RH. The HONO yield is ca. 30% for three different RH 0%, 30%, and 90%, and it is about 20% at 60% RH. In contrast to the HONO yield, a small NO_2 to NO conversion yield was observed on the FL surface (ca. 10%) which was almost independent of the RH. Somewhat higher NO yields were observed in the case of FL/Na_2SO_4 at RH 0% (20%) and RH 30% (40%) which then decrease to 10% at higher RH (60−90%). The total formation of both HONO and NO yields is lower than 50% in dry conditions (RH 0%), while it increased to very high yields with increasing RH, up to 90% at RH 90%.

The products may also involve nonvolatile surface-adsorbed N-containing species because the sum of HONO and NO was always less than 100%. To confirm the presence of the N-containing species, ion analysis was carried out to characterize the ion composition of the glass plates before and after reaction with NO_2 (Table S1).

The obtained qualitative results indicate slight formation of nitric acid/nitrate (HNO_3/NO_3^-) on solid FL film upon light-induced NO_2 heterogeneous reaction at RH 60%, while the formed nitrite (NO_2^-) is nearly below the detection limit. A recent study by Laufs and Kleffmann[40] reported a very low HNO_3 photolysis frequency for HONO formation of $J(HNO_3 \rightarrow HONO)$ = 2.4 × 10^{-7} s^{-1} (0° SZA, 50% RH). Therefore, HNO_3 photolysis cannot explain the significant HONO levels in the daytime atmosphere.[39]

3.6. Reaction Mechanism. In the past, few studies have focused on the heterogeneous reactions between NO_2 and PAHs.[41−43] Here for the first time we evaluate the HONO formation yields upon light-induced heterogeneous NO_2 reaction on solid film consisting of FL and FL/and FL/Na_2SO_4. On the basis of the obtained experimental results, a simplified reaction pathway is proposed in reaction sequence from R-1 to R-10 to explain the photoenhanced HONO formation. It is known that the heterogeneous reaction may proceed via electron transfer between electronically excited states of PAHs and NO_2.[16,25] Here we suggest a mechanism initiated by the excited triplet state of FL ($^3FL^*$)[44] to explain the increase of NO_2 uptakes at higher RH. Electronically excited state of fluorene reacts with the coadsorbed NO_2 in a way that an electron transfer to NO_2 affords a nitrate−FL complex. This complex can later decompose and become a source of nitrate anion (NO_2^-) and FL cation (FL^+), displayed by reactions R-1 to R-3. Moreover, FL^+ in a presence of RH forms a FL−H_2O complex through a hydrogen bond, which through the process of deprotonation yields fluorenol (FL−OH) (R-4 and R-5). Additionally, FL−OH can be easily combined with NO_2^-, leading to the formation of HONO (R-6). However, a competitive reaction, occurring between FL−OH and SO_4^{2-} (R-7), might be a reason for the obvious decrease in HONO formation, as the Na_2SO_4 salt plays a role of inhibitor in HONO production. The acid−base reaction between NO_2^- and H^+ can be also regarded as an additional formation pathway of HONO (R-8). NO_2^- can also photodissociate and generate NO as a byproduct (R-9).

https://dx.doi.org/10.1021/acs.est.0c02627
Environ. Sci. Technol. 2020, 54, 11079−11086

$$FL \xrightarrow{h\nu} {}^3[FL]^* \quad (R1)$$

$${}^3[FL]^* + NO_2 \rightarrow [FL^+ - NO_2^-] \quad (R2)$$

$$[FL^+ - NO_2^-] \rightarrow FL^+ + NO_2^- \quad (R3)$$

$$FL^+ + H_2O \rightarrow FL - OH_2^+ \quad (R4)$$

$$FL - OH_2^+ \xrightarrow[-H^+]{} FL - OH \quad (R5)$$

$$FL - OH + NO_2^- \rightarrow FLO + HONO \quad (R6)$$

$$FL - OH + SO_4^{2-} \rightarrow \text{products} \quad (R7)$$

$$NO_2^- + H^+ \rightleftharpoons HONO \quad (R8)$$

$$NO_2^- \xrightarrow{h\nu} NO + O^- \quad (R9)$$

$$FL^+ + e^- \rightarrow FL \quad (R10)$$

Finally, FL is regenerated through R10. As we mentioned in Material and Methods, we used N_2 as a carrier gas of NO_2, but the use of O_2 as a carrier gas can lead to the formation of $^1O_2$ species on the environmental surfaces which in turn can react with the adsorbed PAHs[45] and eventually affect the HONO formation yields. However, this issue was out of scope of this research study, but in the future the influence of typical carrier gases (N_2, O_2, He) on the reactive uptake coefficients and HONO formation yields should be explored. Also in the future, the role of substrate and charge transfer acceptors in the context of PAH-photosensitized NO_2 heterogeneous chemistry should be evaluated.[16,46]

4. ATMOSPHERIC IMPLICATIONS

The measured geometric uptake coefficients can be used in photochemical models to account for unknown daytime HONO sources in an urban area.[20] The role of FL as a photosensitizer could possibly explain the NO_2 light-induced HONO formation on urban surfaces. Assuming that a street canyon with a surface of 20 m building height and 10 m street width is covered with only 1% by grime consisting of FL, the obtained HONO source strength based on the HONO surface flux (see SI) would yield a HONO production rate of 110 ppt h^{-1} in the "wet season" (RH 90%) and 53 ppt h^{-1} in the "dry season" (RH 30%). These formation rates of HONO can contribute to the missing HONO source in urban environment as indicated by photochemical models.[47,48] Su et al.[49] reported an unknown daytime HONO source in Guangzhou, China, with a maximum of 4900 ppt h^{-1}. High unknown daytime HONO production rates with a maximum of 2500 ppt h^{-1} were reported for the coastal regions of China, in the Beijing–Tianjin–Hebei region.[50] A recent study reported an unknown HONO source of 980 ppt h^{-1} in Xi'an (China), associated with the product of photolysis frequency of NO_2, $J(NO_2)$, and the NO_2 concentration, $[NO_2]$, $J(NO_2)[NO_2]$, indicating that light-induced heterogeneous NO_2 conversion is likely a source of the unknown HONO formation rate.[51]

Considering that PAHs as photosensitizers[52,53] represent an important fraction of urban grime,[8] the results from this study indicate that PAHs play an important role in urban air pollution through light-induced heterogeneous conversion of NO_2 to HONO on urban surfaces. In the future, NO_2 uptakes should be measured in the presence of O_2 as a carrier gas in the reactor which may influence the reaction mechanism of NO_2 and potentially affect the HONO formation yields.

A comprehensive understanding of HONO formation processes is crucial regarding the indoor air, as HONO is the main precursor of hydroxyl radicals (OH) through photolysis of HONO.[54−56] In terms of HONO flux,[20] the light-induced HONO production is 1.5×10^{10} molecules cm^{-2} s^{-1} on a solid film of fluorene under UV irradiation of 15.5 W m^{-2} in the presence of 40 ppb of NO_2 which is comparable with the HONO flux of 1.3×10^{10} and 2.7×10^{10} molecules cm^{-2} s^{-1} produced by light-induced heterogeneous NO_2 to HONO conversion on a white wall with paint and lacquer at 50 ppb of NO_2 and RH of 50%,[26] and 2.5×10^{10} molecules cm^{-2} s^{-1} generated by a light-induced heterogeneous reaction of NO_2 on a soil surface under stronger UV irradiation (70 W m^{-2}) and in the presence of 17 ppb of NO_2.[21] The photochemical models containing currently known and postulated sources of HONO cannot reproduce the observed daytime HONO levels indoors;[57] hence, the suggested light-induced heterogeneous reactions of NO_2 on glass windows containing PAHs such as FL can represent an important additional HONO source in indoor air which may explain the difference between the observed and the modeled HONO values.

■ ASSOCIATED CONTENT

Supporting Information

The Supporting Information is available free of charge at https://pubs.acs.org/doi/10.1021/acs.est.0c02627.

Typical signal of NO_2 and HONO formation on solid film consisting of FL. Additional details on Langmuir–Hinshelwood mechanism. Ion concentrations on the glass plate consisting of FL and FL/Na_2SO_4 before and after reaction with NO_2. Estimation of HONO production in the flow tube reactor (PDF)

■ AUTHOR INFORMATION

Corresponding Author

Sasho Gligorovski − *State Key Laboratory of Organic Geochemistry, Guangzhou Institute of Geochemistry, Chinese Academy of Sciences, Guangzhou 510 640, China;* orcid.org/0000-0003-4151-2224; Phone: +86 2085291497; Email: gligorovski@gig.ac.cn

Authors

Jiangping Liu − *State Key Laboratory of Organic Geochemistry, Guangzhou Institute of Geochemistry, Chinese Academy of Sciences, Guangzhou 510 640, China; University of Chinese Academy of Sciences, Beijing, China*

Huifan Deng − *State Key Laboratory of Organic Geochemistry, Guangzhou Institute of Geochemistry, Chinese Academy of Sciences, Guangzhou 510 640, China; University of Chinese Academy of Sciences, Beijing, China*

Sheng Li − *State Key Laboratory of Organic Geochemistry, Guangzhou Institute of Geochemistry, Chinese Academy of Sciences, Guangzhou 510 640, China; University of Chinese Academy of Sciences, Beijing, China*

Haoyu Jiang − *State Key Laboratory of Organic Geochemistry, Guangzhou Institute of Geochemistry, Chinese Academy of Sciences, Guangzhou 510 640, China*

Majda Mekic − *State Key Laboratory of Organic Geochemistry, Guangzhou Institute of Geochemistry, Chinese Academy of*

https://dx.doi.org/10.1021/acs.est.0c02627
Environ. Sci. Technol. 2020, 54, 11079−11086

Sciences, Guangzhou 510 640, China; University of Chinese Academy of Sciences, Beijing, China; orcid.org/0000-0001-7241-1827

Wentao Zhou − *State Key Laboratory of Organic Geochemistry, Guangzhou Institute of Geochemistry, Chinese Academy of Sciences, Guangzhou 510 640, China; University of Chinese Academy of Sciences, Beijing, China*

Yiqun Wang − *State Key Laboratory of Organic Geochemistry, Guangzhou Institute of Geochemistry, Chinese Academy of Sciences, Guangzhou 510 640, China; University of Chinese Academy of Sciences, Beijing, China*

Gwendal Loisel − *State Key Laboratory of Organic Geochemistry, Guangzhou Institute of Geochemistry, Chinese Academy of Sciences, Guangzhou 510 640, China*

Xinming Wang − *State Key Laboratory of Organic Geochemistry, Guangzhou Institute of Geochemistry, Chinese Academy of Sciences, Guangzhou 510 640, China;* orcid.org/0000-0002-1982-0928

Complete contact information is available at: https://pubs.acs.org/10.1021/acs.est.0c02627

Notes

The authors declare no competing financial interest.

■ ACKNOWLEDGMENTS

This work was supported by National Natural Science Foundation of China (no. 41773131, no. 41977187) and State Key Laboratory of Organic Geochemistry, Guangzhou Institute of Geochemistry (no. SKLOG2020-5).

■ REFERENCES

(1) Baergen, A. M.; Styler, S. A.; Van Pinxteren, D.; Müller, K.; Herrmann, H.; Donaldson, D. J. Chemistry of Urban Grime: Inorganic Ion Composition of Grime vs Particles in Leipzig, Germany. *Environ. Sci. Technol.* **2015**, *49* (21), 12688−12696.

(2) Baergen, A. M.; Donaldson, D. J. Formation of reactive nitrogen oxides from urban grime photochemistry. *Atmos. Chem. Phys.* **2016**, *16*, 6355−6363.

(3) Styler, S. A.; Baergen, A. M.; Donaldson, D. J.; Herrmann, H. Organic Composition, Chemistry, and Photochemistry of Urban Film in Leipzig, Germany. *ACS Earth Space Chem.* **2018**, *2* (9), 935−945.

(4) Diamond, M. L.; Gingrich, S. E.; Fertuck, K.; McCarry, B. E.; Stern, G. A.; Billeck, B.; Grift, B.; Brooker, D.; Yager, T. D. Evidence for organic film on an impervious urban surface: characterization and potential teratogenic effects. *Environ. Sci. Technol.* **2000**, *34*, 2900−2908.

(5) Lam, B.; Diamond, M. L.; Simpson, A. J.; Makar, P. A.; Truong, J.; Hernandez-Martinez, N. A. Chemical composition of surface films on glass windows and implications for atmospheric chemistry. *Atmos. Environ.* **2005**, *39* (35), 6578−6586.

(6) Gingrich, S. E.; Diamond, M. L.; et al. Atmospherically derived organic surface films along an urban-rural gradient. *Environ. Sci. Technol.* **2001**, *35*, 4031−4037.

(7) Simpson, A. J.; Lam, B.; Diamond, M. L.; Donaldson, D. J.; Lefebvre, B. A.; Moser, A. Q.; Williams, A. J.; Larin, N. I.; Kvasha, M. P. Assessing the organic composition of urban surface films using nuclear magnetic resonance spectroscopy. *Chemosphere* **2006**, *63* (1), 142−152.

(8) Pan, S. H.; Li, J.; Lin, T.; Zhang, G.; Li, X. D.; Yin, H. Polycyclic aromatic hydrocarbons on indoor/outdoor glass window surfaces in Guangzhou and Hong Kong, south China. *Environ. Pollut.* **2012**, *169*, 190−195.

(9) Unger, M.; Gustafsson, O. PAHs in Stockholm window films: evaluation of the utility of window film content as indicator of PAHs in urban air. *Atmos. Environ.* **2008**, *42* (22), 5550−5557.

(10) Barbas, J. T.; Sigman, M. E.; Dabestani, R. Dabestani, R, Photochemical Oxidation of Phenanthrene Sorbed on Silica Gel. *Environ. Sci. Technol.* **1996**, *30*, 1776−1780.

(11) Barbas, J. T.; Sigman, M. E.; Arce, R.; Dabestani, R. Spectroscopy and photochemistry of fluorene at a silica gel/air interface. *J. Photochem. Photobiol., A* **1997**, *109*, 229−236.

(12) Chabas, A.; Lombardo, T.; Cachier, H.; Pertuisot, M. H.; Oikonomou, K.; Falcone, R.; Verità, M.; Geotti-Bianchini, F. Behaviour of Self-Cleaning Glass in Urban Atmosphere. *Build Environ.* **2008**, *43* (12), 2124−2131.

(13) Ma, Q.; He, H.; Liu, Y.; Liu, C.; Grassian, V. H. Heterogeneous and multiphase formation pathways of gypsum in the atmosphere. *Phys. Chem. Chem. Phys.* **2013**, *15*, 19196−19204.

(14) Baergen, A. M.; Donaldson, D. J. Photochemical renoxification of nitric acid on real urban grime. *Environ. Sci. Technol.* **2013**, *47*, 815−820.

(15) George, C.; Strekowski, R. S.; Kleffmann, J.; Stemmler, K.; Ammann, M. Photoenhanced uptake of gaseous NO_2 on solid organic compounds: a photochemical source of HONO? *Faraday Discuss.* **2005**, *130*, 195−210.

(16) Brigante, M.; Cazoir, D.; D'Anna, B.; George, C.; Donaldson, D. J. Photoenhanced Uptake of NO_2 by Pyrene Solid Films. *J. Phys. Chem. A* **2008**, *112*, 9503−9508.

(17) Ammar, R.; Monge, M. E.; George, C.; D'Anna, B. Photoenhanced NO_2 Loss on Simulated Urban Grime. *ChemPhysChem* **2010**, *11*, 3956−3961.

(18) Sosedova, Y.; Rouvière, A.; Bartels-Rausch, T.; Ammann, M. UVA/Vis-induced nitrous acid formation on polyphenolic films exposed to gaseous NO_2. *Photochem. Photobiol. Sci.* **2011**, *10*, 1680−1690.

(19) Cazoir, D.; Brigante, M.; Ammar, R.; D'Anna, B.; George, C. Heterogeneous Photochemistry of Gaseous NO_2 on Solid Fluoranthene Films: A Source of Gaseous Nitrous Acid (HONO) in the Urban Environment. *J. Photochem. Photobiol., A* **2014**, *273*, 23−28.

(20) Liu, J. P.; Li, S.; Mekic, M.; Jiang, H. Y.; Zhou, W. T.; Loisel, G.; Song, W.; Wang, X. M.; Gligorovski, S. Photoenhanced uptake of NO_2 and HONO formation on real urban grime. *Environ. Sci. Technol. Lett.* **2019**, *6*, 413−417.

(21) Stemmler, K.; Ammann, M.; Donders, C.; Kleffmann, J.; George, C. Photosensitized reduction of nitrogen dioxide on humic acid as a source of nitrous acid. *Nature* **2006**, *440*, 195−198.

(22) Stemmler, K.; Ndour, M.; Elshorbany, Y.; Kleffmann, J.; D'Anna, B.; George, C.; Bohn, B.; Ammann, M. Light induced conversion of nitrogen dioxide into nitrous acid on submicron humic acid aerosol. *Atmos. Chem. Phys.* **2007**, *7*, 4237−4248.

(23) Ndour, M.; D'Anna, B.; George, C.; Ka, O.; Balkanski, Y.; Kleffmann, J.; Stemmler, K.; Ammann, M. Photoenhanced uptake of NO_2 on mineral dust: Laboratory experiments and model simulations. *Geophys. Res. Lett.* **2008**, *35*, L05812.

(24) Monge, M. E.; D'Anna, B.; George, C. Nitrogen dioxide removal and nitrous acid formation on titanium oxide surfaces-an air quality remediation process? *Phys. Chem. Chem. Phys.* **2010**, *12*, 8991−8998.

(25) Monge, M. E.; D'Anna, B.; Mazri, L.; Giroir-Fendler, A.; Ammann, M.; Donaldson, D. J.; George, C. Light changes the atmospheric reactivity of soot. *Proc. Natl. Acad. Sci. U. S. A.* **2010**, *107*, 6605−6609.

(26) Gómez Alvarez, E.; Soergel, M.; Gligorovski, S.; Bassil, S.; Bartolomei, V.; Coulomb, B.; Zetzsch, C.; Wortham, H. Light-induced nitrous acid (HONO) production from NO_2 heterogeneous reactions on household chemicals. *Atmos. Environ.* **2014**, *95*, 391−399.

(27) Gandolfo, A.; Bartolomei, V.; Gómez Alvarez, E.; Tlili, S.; Gligorovski, S.; Kleffmann, J.; Wortham, H. The effectiveness of indoor photocatalytic paints on NOx and HONO levels. *Appl. Catal., B* **2015**, *166*−*167*, 84−90.

(28) Gandolfo, A.; Rouyer, L.; Wortham, H.; Gligorovski, S. The influence of wall temperature on NO_2 removal and HONO levels

released by indoor photocatalytic paints. *Appl. Catal., B* **2017**, *209*, 429−436.
(29) Gandolfo, A.; Bartolomei, V.; Truffier-Boutry, D.; Temime-Roussel, B.; Brochard, G.; Bergé, V.; Wortham, H.; Gligorovski, S. The impact of photocatalytic paint's porosity on indoor NOx and HONO levels. *Phys. Chem. Chem. Phys.* **2020**, *22*, 589−598.
(30) Ma, J.; Liu, Y.; Han, C.; Ma, Q.; Liu, C.; He, H. Review of heterogeneous photochemical reactions of NOy on aerosol − A possible daytime source of nitrous acid (HONO) in the atmosphere. *J. Environ. Sci.* **2013**, *25*, 326−334.
(31) Heland, J.; Kleffmann, J.; Kurtenbach, R.; Wiesen, P. A New instrument to measure gaseous nitrous acid (HONO) in the atmosphere. *Environ. Sci. Technol.* **2001**, *35*, 3207−3212.
(32) Snellinx, Z.; et al. Biological remediation of explosives and related nitroaromatic compounds. *Environ. Sci. Pollut. Res.* **2002**, *9* (1), 48−61.
(33) Kleffmann, J.; Wiesen, P. Technical Note: Quantification of interferences of wet chemical HONO LOPAP measurements under simulated polar conditions. *Atmos. Chem. Phys.* **2008**, *8*, 6813−6822.
(34) Behnke, W.; George, C.; Scheer, V.; Zetzsch, C. Production and decay of ClONO2 from the reaction of gaseous N2O5 with NaCl solution: bulk and aerosol experiments. *J. Geophys. Res.* **1997**, *102* (D3), 3795−3804.
(35) Madronich, S. Photodissociation in the atmosphere 1. Actinic flux and the effect of ground reflections and clouds. *J. Geophys. Res.* **1987**, *92*, 9740−9752.
(36) Arens, F.; Gutzwiller, L.; Gaggeler, H. W.; Ammann, M. The reaction of NO_2 with solid anthrarobin (1,2,10-trihydroxyanthracene). *Phys. Chem. Chem. Phys.* **2002**, *4*, 3684−3690.
(37) Mekic, M.; Loisel, G.; Zhou, W.; Jiang, B.; Vione, D.; Gligorovski, S. Ionic strength effects on the reactive uptake of ozone on aqueous pyruvic acid: Implications for air-sea ozone deposition. *Environ. Sci. Technol.* **2018**, *52*, 12306−12315.
(38) National Renewable Energy Laboratory (NREL), American Society for Testing and Materials G-173−03 Reference Spectra, https://rredc.nrel.gov/solar//spectra/am1.5/. 2003.
(39) Han, C.; Yang, W.; Wu, Q.; Yang, H.; Xue, X. Heterogeneous photochemical conversion of NO2 to HONO on humic acid surface under simulated sunlight. *Environ. Sci. Technol.* **2016**, *50*, 5017−5023.
(40) Laufs, S.; Kleffmann, J. Investigations on HONO formation from photolysis of adsorbed HNO_3 on quartz glass surfaces. *Phys. Chem. Chem. Phys.* **2016**, *18*, 9616−9625.
(41) Pitts, J. N., Jr.; Van Cauwenberghe, K. A.; Grosjean, D.; Schmid, J. P.; Fitz, D. R.; Belser, W. L., Jr; Knudson, G. B.; Hynds, P. M. Atmospheric reactions of polycyclic aromatic hydrocarbons: facile formation of mutagenic nitro derivatives. *Science* **1978**, *202*, 515−519.
(42) Perraudin, E.; Budzinski, H.; Villenave, E. Kinetic study of the reactions of NO_2 with polycyclic aromatic hydrocarbons adsorbed on silica particles. *Atmos. Environ.* **2005**, *39*, 6557−6567.
(43) Esteve, W.; Budzinski, H.; Villenave, E. Relative rate constants for the heterogeneous reactions of NO_2 and OH radicals with polycyclic aromatic hydrocarbons adsorbed on carbonaceous particles. Part 2. PAHs adsorbed on diesel particulate exhaust SRM 1650. *Atmos. Environ.* **2006**, *40*, 201−211.
(44) Mekic, M.; Zeng, J.; Jiang, B.; Li, X.; Lazarou, Y. G.; Brigante, M.; Herrmann, H.; Gligorovski, S. Formation of toxic unsaturated multifunctional and organosulfur compounds from the photosensitized processing of fluorene and DMSO at the air-water interface. *J. Geophys. Res.: Atmos.* **2020**, *125*, No. e2019JD031839.
(45) Cote, C. D.; Schneider, S. R.; Lyu, M.; Gao, S.; Gan, L.; Holod, A. J.; Chou, T. H. H; Styler, S. A. Photochemical Production of Singlet Oxygen by Urban Road Dust. *Environ. Sci. Technol. Lett.* **2018**, *5*, 92−97.
(46) Styler, S. A.; Loiseaux, M.-E.; Donaldson, D. J. Substrate effects in the photoenhanced ozonation of pyrene. *Atmos. Chem. Phys.* **2011**, *11*, 1243−1253.
(47) Lee, J. D.; Whalley, L. K.; Heard, D. E.; Stone, D.; Dunmore, R. E.; Hamilton, J. F.; Young, D. E.; Allan, J. D.; Laufs, S.; Kleffmann, J. Detailed budget analysis of HONO in central London reveals a missing daytime source. *Atmos. Chem. Phys.* **2016**, *16*, 2747−2764.
(48) Zhang, J.; An, J.; Qu, Y.; Liu, X.; Chen, Y. Impacts of potential HONO sources on the concentrations of oxidants and secondary organic aerosols in the Beijing-Tianjin-Hebei region of China. *Sci. Total Environ.* **2019**, *647*, 836−852.
(49) Su, H.; Cheng, Y. F.; Shao, M.; Gao, D. F.; Yu, Z. Y.; Zeng, L. M.; Slanina, J.; Zhang, Y. H.; Wiedensohler, A. Nitrous acid (HONO) and its daytime sources at a rural site during the 2004 PRIDE-PRD experiment in China. *J. Geophys. Res.* **2008**, *113*, D14312.
(50) Tang, Y.; An, J.; Wang, F.; Li, Y.; Qu, Y.; Chen, Y.; Lin, J. Impacts of an unknown daytime HONO source on the mixing ratio and budget of HONO, and hydroxyl, hydroperoxyl, and organic peroxy radicals, in the coastal regions of China. *Atmos. Chem. Phys.* **2015**, *15*, 9381−9398.
(51) Huang, R. J.; Yang, L.; Cao, J.; Wang, Q.; Tie, X.; Ho, K. F.; Shen, Z.; Zhang, R.; Li, G.; Zhu, C.; Zhang, N.; Dai, W.; Zhou, J.; Liu, S.; Chen, Y.; Chen, J.; O'Dowd, C. D. Concentration and sources of atmospheric nitrous acid (HONO) at an urban site in Western China. *Sci. Total Environ.* **2017**, *593-594*, 165−172.
(52) Gómez Alvarez, E.; Wortham, H.; Strekowski, R.; Zetzsch, C.; Gligorovski, S. Atmospheric photo-sensitized heterogeneous and multiphase reactions: From outdoors to indoors. *Environ. Sci. Technol.* **2012**, *46*, 1955−1963.
(53) Vione, D.; Maurino, V.; Minero, C.; Pelizzetti, E.; Harrison, M. A. J.; Olariu, R. I.; Arsene, C. Photochemical reactions in the tropospheric aqueous phase and on particulate matter. *Chem. Soc. Rev.* **2006**, *35*, 441−453.
(54) Gómez Alvarez, E.; Amedro, D.; Afif, C.; Gligorovski, S.; Schoemacker, C.; Fittschen, C.; Doussin, J. F.; Wortham, H. Unexpectedly high indoor hydroxyl radical concentrations associated with nitrous acid. *Proc. Natl. Acad. Sci. U. S. A.* **2013**, *110* (33), 13294−13299.
(55) Bartolomei, V.; Gómez Alvarez, E.; Wittmer, J.; Tlili, S.; Strekowski, R.; Temime-Roussel, B.; Quivet, E.; Wortham, H.; Zetzsch, C.; Kleffmann, J.; Gligorovski, S. Combustion processes as a source of high levels of indoor hydroxyl radical (OH) through the photolysis of nitrous acid (HONO). *Environ. Sci. Technol.* **2015**, *49* (11), 6599−6607.
(56) Liu, J.; Li, S.; Zeng, J.; Mekic, M.; Yu, Z.; Zhou, W.; Loisel, G.; Gandolfo, A.; Song, W.; Wang, X.; Zhou, Z.; Herrmann, H.; Li, X.; Gligorovski, S. Assessing indoor gas phase oxidation capacity through real-time measurements of HONO, NOx and ozone in Guangzhou, China. *Environ. Environ. Sci.: Processes Impacts.* **2019**, *21*, 1393−1402.
(57) Mendez, M.; Amedro, D.; Blond, N.; Hauglustaine, D.; Blondeau, P.; Afif, C.; Fittschen, C.; Schoemaecker, C. Identification of the major HOX radical pathways in an indoor air environment. *Indoor Air.* **2017**, *27*, 434−442.

https://dx.doi.org/10.1021/acs.est.0c02627
Environ. Sci. Technol. 2020, 54, 11079−11086